

A sensitivity approach for computation of the probability density function of critical clearing time and probability of stability in power system transient stability analysis

Saffet Ayasun^{a,*}, Yiqiao Liang^b, Chika O. Nwankpa^c

^a Department of Electrical and Electronics Engineering, Nigde University, 51200 Nigde, Turkey

^b ALSTOM Drives & Controls, Pittsburgh, PA 15238, USA

^c Department of Electrical and Computer Engineering, Drexel University, Philadelphia, PA 1904, USA

Abstract

This paper presents a linear approximation method to determine the probability density function (PDF) of the critical clearing time (CCT) and probability of stability for a given disturbance in power system transient stability analysis. The CCT is the maximum time interval by which the fault must be cleared in order to preserve the system stability. The CCT depends on the system load level and thus, is modeled as a random variable due to the probabilistic nature of system load demand. The proposed method first determines the sensitivity of the CCT with respect to the system load, and using these sensitivities it computes the PDF of the CCT based on the PDF of the system load. The probability of system being transiently stable for a particular disturbance and for a given fault clearing time is calculated using the PDF of CCT. This approach is verified to be accurate under the condition of small load deviation by Monte Carlo simulations method. Moreover, the proposed method reduces the computational effort significantly in Monte Carlo simulations indicating that it could be used in real-time on-line applications.

© 2005 Elsevier Inc. All rights reserved.

Keywords: Electric power system; Transient stability; Critical clearing time; Linearization; Probability density function; Probability of stability

1. Introduction

Transient stability assessment is a major requirement for safe operation of power systems. The transient stability is analyzed considering the effect on the system of large disturbances such as faults, loss of loads or generators, line switching, etc. A power system is *transiently stable* for a particular steady-state operating condition and for a particular large disturbance if, following that disturbance; it reaches an acceptable

* Corresponding author.

E-mail addresses: saffet@nwankpa.ece.drexel.edu, sayasun@nigde.edu.tr (S. Ayasun), liang@gegelec.com (Y. Liang), chika@nwankpa.ece.drexel.edu (C.O. Nwankpa).

steady-state operating condition [1]. The time domain simulations and direct methods are the two methods commonly used in transient stability studies. The time domain simulation method solves the differential-algebraic equations that describe the power system dynamics under different faulted conditions in order to find out if the system will preserve its stability. The method suffers in its slow speed and inability to provide an index that enables to measure the degree of stability of the system quantitatively.

Direct methods, on the other hand, employing energy functions provide a stability index that gives stability margin of an operating point in terms of energy stored in the system [2–4]. There are several variants of the direct method such as potential energy boundary surface (PEBS) method [5]; boundary of stability region based controlling unstable equilibrium point (BCU) method [6] and equal area criterion (EAC) [7–9]. The main objective of the various direct methods is to determine the critical fault clearing time and the corresponding critical energy value without solving the system differential equations in order to assess the transient stability of the system. The critical clearing time (CCT) is the maximum time interval by which the fault must be cleared in order to preserve the system stability. In direct stability assessment methods, the CCT is calculated and compared with the actual fault clearing time. If the former is greater than the latter the system is determined to be transiently stable. The difference between these two values can be used as an index to quantify the degree of system stability. A higher value of this index indicates a more stable system. The difference between the critical energy value and the energy at the fault clearing time is sometimes employed as an index as well. Even though the direct methods have drastically improved the program speed, the size of electrical power systems and the complexity of the transient stability problem still involve prohibitive calculations. With the advent of more advanced algorithms and faster computers, transient stability study has been implemented in Energy Management System (EMS) for real-time on-line operation. Like many other application programs in the EMS system [10], the transient stability program (TSP) is continually executed in a certain interval of time. Depending on the computing power of the EMS system, this interval can range from tens of minutes to an hour. The execution flow of this program is illustrated in Fig. 1.

At time t_k TSP is started and it gets a snapshot of system data such as load level and equipment parameters at this instant of time and performs necessary calculations to determine the CCT. After Δt amount of time, the program terminates and conclusions regarding the system transient stability are obtained. At time t_{k+1} the above procedure will be repeated. The system data captured at time t_k or t_{k+1} reflects the steady-state operating condition of the system and parameters. Among those, the load level is one of the parameters that heavily affects the stability. In other words, the stability of the system or equivalently, the critical clearing time (CCT) is a function of the system load level. Thus, the conclusions drawn based on the system load at time t_k will not always hold true from $t_k + \Delta t$ to t_{k+1} due to the fact that the system load keeps changing in actual operation. Therefore, the CCT should be modeled as a random variable in order to take into account the random nature of the system load. Based on the arguments above, a system being transiently stable under a particular contingency is also a random event. The information on the probability of this random event is crucial for power system planning studies and safe operation. Under the assumption that the probability density function (PDF) of the CCT is known, the probability of the system being transiently stable can be calculated by

$$P\{\text{system being stable}\} = P\{t_c < t_{cc}\}, \quad (1)$$

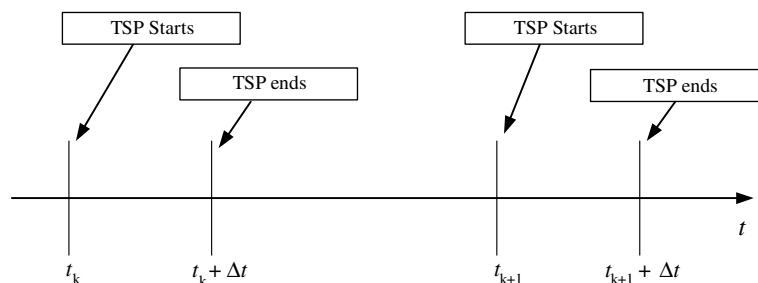


Fig. 1. TSP execution flow in the EMS system.

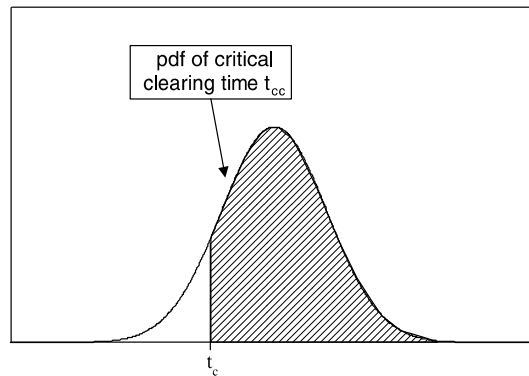


Fig. 2. Graphical illustration of the probability of system being transient stable.

where t_c and t_{cc} are the actual fault clearing time and critical clearing time, respectively. The shaded area in Fig. 2 graphically shows this probability value. For illustrative purposes, the CCTs are assumed to be normally distributed in Fig. 2.

The necessity of the probabilistic assessment of the power transient stability has been widely recognized as pointed out in [11]. There are two main methods in the literature for probabilistic assessment of transient stability. The first method employs the conditional probability approach to evaluate the probability of stability analytically [12–20]. The second utilizes Monte Carlo simulation approach to estimate the probability of stability [21,22]. Billinton and Kurunganty [12] developed a single stability index that takes into account the probabilistic aspects of fault type, fault location, fault clearing time and system operating conditions, and applied it to a practical 33-bus power system [13]. Hsu and Chang [14] used the conditional probability approach to carry out a transient stability analysis on the Taiwan power system deriving joint probability distribution of the CCT using the system outage statistics. In [15–17] Chiodo and his co-workers developed an approximate method to determine the probability of stability as a function of the CCT. They proposed an analytical and invertible log-linear functional relationship between the CCT and the system load. Such an approximation enables the analytical computation of both the PDF of the CCT in terms of PDF of the system load and probability of instability. In [18], the bisection algorithm has been employed to reduce the amount of computation time required in the probabilistic evaluation of transient stability. More recent publications [19,20] have reported on-line implementation of the probabilistic transient stability analysis that employs the conditional probability approach.

The core of the analytical approaches mentioned above is the analytical computation of the PDF of the CCT in terms of the PDF of the load. In principle, once the PDF of the system load is known, the PDF of the CCT can be obtained by using well known theorems on random variable transformations [23]. The PDF of the system load can be determined from the historical data of the Supervisory Control and Data Acquisition (SCADA) system. However, as will be shown later in the paper, the CCT is a complicated function of the system load as well as other parameters including voltages, reactances, etc. In other words, the function that relates the CCT to the system load is not analytically invertible. Therefore, the PDF of the CCT can not be obtained analytically in a closed-form expression. In such cases, either the functional dependency between the CCT and load is approximately described by a simpler, invertible, analytical function or Monte Carlo simulations method is used to estimate the PDF of the CCT [21,22] without making simplifying assumptions. The Monte Carlo method is suitable for the analysis of complicated events and does not put any restriction on the mathematical model used. However, it requires a lot of computational effort to obtain the PDF of the CCT. The computational effort becomes even more significant when a large number of samples are used to improve the accuracy of the estimated probability. Hence, it might not be appropriate for on-line transient stability analysis.

This paper presents a linear approximation method to determine the probability density function (PDF) of the critical clearing time (CCT) and probability of stability for a given disturbance. The CCT is approximately described by a linear function of the system load using the sensitivity of the CCT with respect to the load. It

has been shown that analytical calculation of the sensitivity of the CCT to the rotor angle, which is also a function of the load, is not straightforward and it brings some computational difficulties. Therefore, a new formula is derived to overcome the difficulty of calculating this sensitivity, which is a significant contribution of this work. The system loads are assumed to be normally distributed. Using the proposed linear relationship between the CCT and load, Monte Carlo simulations are carried out to estimate the PDF of the CCT based on the load PDF and to validate the accuracy of the proposed linear approximation. The probability of system being transiently stable for a particular disturbance and for a given fault clearing time is calculated using the PDF of CCT. The exact and approximated PDF of CCTs and probability of stabilities are compared for two different cases of a One-Machine-Infinite-Bus (OMIB) power system. The results show that the linear approximation is valid and give adequately accurate results under the condition of small load deviations. More importantly, the proposed method reduces the computational effort significantly in Monte Carlo simulations indicating that it could be used in real-time on-line applications.

2. Problem formulation

In transient stability studies using direct methods, the multi-machine power system is reduced to a one-machine-infinite-bus (OMIB) system [24–26]. A graphical method known as equal area criterion (EAC) is applied to the OMIB system to compute critical clearing time and to assess the system stability for a given fault scenario. In this section, the EAC method will be revisited to establish the relationship between the critical clearing time and system load. With the inherent errors involved in reducing a power system model to an equivalent OMIB system, modeling fluctuations in load become even more necessary.

2.1. Swing equation

Fig. 3 shows an OMIB system where a generator is connected to an infinite bus through a transformer and two parallel transmission lines. The infinite bus at a constant voltage V represents the rest of the power system. The machine (generator) is represented by a reduced order dynamic model characterized by a constant voltage E behind the transient reactance x'_d . The transformer is modeled using a reactance x_t . The differential equation that describes the dynamic behavior of the OMIB system in Fig. 3 can be given as [27]

$$M \frac{d^2\delta}{dt^2} = P_m - P_e, \tag{2}$$

where δ is the generator rotor angle or power angle (rad), M is the moment of inertia of the generator, P_m is the generator mechanical power (pu) that represents the system load at the equilibrium point, $P_e = P_{max} \sin \delta$ is the electrical power transferred by the generator to the system represented by the infinite bus (pu). The $P_e(\delta)$ is called the power-angle curve and its maximum value is $P_{max} = \frac{EV}{x}$ with $x = x'_d + x_t + \frac{x_r}{2}$ representing the total equivalent reactance between the generator and the infinite bus (pu). The nonlinear differential equation given in (2) is called the *swing equation* because it describes swings in power angle δ during transients.

In this study, the following fault scenario is assumed. At a given time of t , a three-phase to ground fault occurs on one of the transmission lines while the OMIB system is operating at a pre-fault stable equilibrium point. The fault location is labeled by (X) in Fig. 3. The fault is not cleared instantaneously by the circuit breakers and the generator continues transferring power during the fault-on conditions. At $t = t_c$, the fault

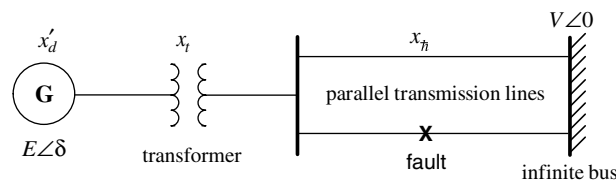


Fig. 3. One-machine-infinite-bus (OMIB) system.

is cleared and the faulted line is isolated (removed). After the fault is cleared (post-fault condition), the system transfers power using one good transmission line in place.

For the given fault scenario above and clearing time t_c , the stability of the OMIB system can be determined by either integrating the nonlinear swing equation of (2) numerically or using equal area criterion (EAC). The EAC is a graphical method to find out the stability of the system under transient conditions without solving the swing equation. The EAC method utilizes power-angle curves to represent the energy stored in the machine during the fault in terms of area under the power-angle curve. Fig. 4 shows power-angle curves for pre-fault, fault-on and post-fault conditions. The maximum value of power transferred for each condition is denoted by $P_{\max 1}$, $P_{\max 2}$ and $P_{\max 3}$, respectively. In this figure, δ_0 is the pre-fault stable operating power angle δ_3 is the post-fault stable operating power angle and δ_c is the fault clearing angle. The values of δ_0 and δ_3 at the equilibrium point are deduced from the swing equation of (2) since the swing equations holds true for pre-fault, fault-on, and post-fault conditions:

$$\delta_0 = \sin^{-1}\left(\frac{P_m}{P_{\max 1}}\right), \tag{3}$$

$$\delta_3 = \sin^{-1}\left(\frac{P_m}{P_{\max 3}}\right). \tag{4}$$

2.2. Equal-area criterion: critical clearing angle and time

The EAC criterion is a graphical method that compares the amount of accelerating energy during the fault-on stage with the amount of decelerating energy after the fault is cleared. The fault-on stage corresponds to power angle interval from pre-fault power angle δ_0 to the fault clearing angle δ_c . Fig. 4 illustrates that during the fault-on stage P_m is greater than the electrical power transferred P_e , which causes the rotor accelerate (i.e., the angle δ increases). The area A in Fig. 4 is the accelerating area representing the kinetic energy stored in the machine because of acceleration of the rotor angle during fault-on stage. The area B is the decelerating area representing the maximum amount of energy that could be absorbed by the system after the fault is cleared. The two areas are defined as follows:

$$\text{Area A} = \int_{\delta_0}^{\delta_c} (P_m - P_{\max 2} \sin \delta) d\delta; \quad \text{Area B} = \int_{\delta_c}^{\pi - \delta_3} (P_{\max 3} \sin \delta - P_m) d\delta. \tag{5}$$

According the EAC, if the area A is less than the area B, then the system is transiently stable. In terms of energy, this condition implies that the system will be able absorb the excess kinetic energy stored in the rotor during the fault-on stage. When the clearing angle is increased to a certain level such that area A is equal

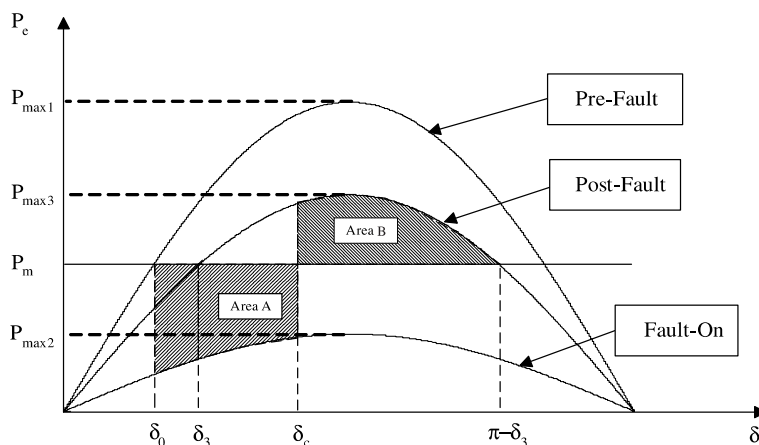


Fig. 4. Pre-fault, fault-on, and post-fault power-angle curves.

to *area B* the system is at a boundary condition. Under this boundary condition, the clearing angle is called the critical clearing angle denoted as δ_{cc} . In other words, critical clearing angle is defined as the maximum power angle such that when the fault is cleared before this angle the system is transiently stable. An expression for critical clearing time is obtained by equating *area A* to *area B*:

$$\delta_{cc} = \cos^{-1} \left[\frac{P_m(\pi - \delta_3 - \delta_0) - P_{\max 3} \cos \delta_3 - P_{\max 2} \cos \delta_0}{P_{\max 3} - P_{\max 2}} \right]. \quad (6)$$

The application of EAC gives the critical clearing angle to maintain stability. However, because of the non-linearity of the swing equation of (2) an analytical solution for critical clearing time is not possible. The critical clearing time is the time when the power angle reaches the critical clearing angle during the first swing. After some manipulations of (2), this critical clearing time can be obtained by

$$t_{cc} = \int_{\delta_0}^{\delta_{cc}} f(\delta, \delta_0) d\delta, \quad (7)$$

where

$$f(\delta, \delta_0) = \frac{1}{\sqrt{\frac{2}{M}(P_m(\delta - \delta_0) + P_{\max 2}(\cos \delta - \cos \delta_0))}}. \quad (8)$$

Equations from (3)–(8) imply that the critical clearing time t_{cc} is a complicated function of system load P_m . This functional dependency between t_{cc} and P_m is synthetically described by a function F as

$$t_{cc} = F(\delta_0(P_m), \delta_{cc}(P_m), P_m). \quad (9)$$

Note that the function F is not simple and analytically invertible. Therefore, using the probability theory, it is not possible to obtain a closed-form expression for the PDF of the t_{cc} analytically in terms of the PDF of the load P_m . Monte Carlo simulations could be utilized for this purpose. However, it requires a lot of computational effort to obtain the PDF of t_{cc} based on the PDF of system load, P_m since Eq. (7) must be numerically integrated for each load value. Hence, it might not be appropriate for on-line transient stability analysis. However, in the following section, an approximate method is proposed for the purpose of real-time applications. The method linearizes Eq. (9) around a stable operating point to determine the sensitivity of the critical clearing time t_{cc} to system load P_m , and utilizes this sensitivity information to develop linear relationship between t_{cc} and P_m .

3. Linear approximation

The critical clearing time t_{cc} is a function of the system load P_m as shown in (9). It is well known that power systems always experience small deviations in load during the normal operating conditions. Hence, a linear approximation of the critical clearing time can easily be obtained by determining the sensitivity the critical clearing time t_{cc} with respect to the system load P_m as follows:

$$t_{cc} = t_{cc0} + \left. \frac{dt_{cc}}{dP_m} \right|_{P_m=P_{m0}} (P_m - P_{m0}), \quad (10)$$

where P_{m0} is the system load at the stable operating point and t_{cc0} is the critical clearing time for this operating point. The key issue in this linear approximation method lies in the calculation of the sensitivity of the critical clearing time to the system load, $\frac{dt_{cc}}{dP_m}$. Applying the chain rule of differentiation to (9), this sensitivity can be expressed as

$$\frac{dt_{cc}}{dP_m} = \frac{\partial F}{\partial \delta_0} \frac{d\delta_0}{dP_m} + \frac{\partial F}{\partial \delta_{cc}} \frac{d\delta_{cc}}{dP_m} + \frac{\partial F}{\partial P_m}. \quad (11)$$

As shown in (11), there are five derivative terms that compose this sensitivity. Four of these terms can be easily obtained as:

$$\frac{d\delta_0}{dP_m} = \frac{1}{P_{\max 1} \cos \delta_0}, \tag{12}$$

$$\begin{aligned} \frac{d\delta_{cc}}{dP_m} = & -\frac{1}{(P_{\max 3} - P_{\max 2}) \sin \delta_{cc}} \left[(\pi - \delta_3 - \delta_0) + \frac{P_{\max 2}}{P_{\max 1}} \tan \delta_0 \right. \\ & \left. + \tan \delta_3 - P_m \left(\frac{1}{P_{\max 1} \cos \delta_0} + \frac{1}{P_{\max 3} \cos \delta_3} \right) \right], \end{aligned} \tag{13}$$

$$\frac{\partial F}{\partial P_m} = \frac{1}{M} \int_{\delta_0}^{\delta_{cc}} (\delta_0 - \delta) f^3(\delta, \delta_0) d\delta, \tag{14}$$

$$\frac{\partial F}{\partial \delta_{cc}} = f(\delta_{cc}, \delta_0). \tag{15}$$

Leibnitz’s rule of differentiation of integral given below could be used to obtain the last derivative term $\partial F/\partial \delta_0$:

$$\frac{\partial}{\partial \alpha} \left[\int_p^q G(x, \alpha) \right] = \int_p^q \frac{\partial G(x, \alpha)}{\partial \alpha} dx + G(q, \alpha) \frac{dq}{d\alpha} - G(p, \alpha) \frac{dp}{d\alpha}. \tag{16}$$

Applying (16) to (7) the following expression is obtained:

$$\frac{\partial}{\partial \delta_0} \left[\int_{\delta_0}^{\delta_{cc}} f(\delta, \delta_0) d\delta \right] = \int_{\delta_0}^{\delta_{cc}} \frac{\partial f(\delta, \delta_0)}{\partial \delta_0} d\delta + f(\delta_{cc}, \delta_0) \frac{d\delta_{cc}}{d\delta_0} - f(\delta_0, \delta_0). \tag{17}$$

However, it must be noted that (17) is not valid and could not be evaluated at $\delta = \delta_0$ because (8) indicates that $\lim_{\delta \rightarrow \delta_0} f(\delta, \delta_0) \rightarrow \infty$. Therefore, a new formula must be developed to compute $\partial F/\partial \delta_0$. The following section gives this new formula and its derivation.

4. A new formula to compute $\partial F/\partial \delta_0$

Proposition. *The derivative of a given function*

$$G(x) = \int_x^a f(t, x) dt \tag{18}$$

with respect to x can be determined by

$$\frac{dG(x)}{dx} = -f(a, x) + \int_x^a \left[\frac{\partial f(z, x)}{\partial z} + \frac{\partial f(z, x)}{\partial x} \right] dz \tag{19}$$

given that $f(a, x)$ and $\int_x^a \left[\frac{\partial f(z, x)}{\partial z} + \frac{\partial f(z, x)}{\partial x} \right] dz$ exist.

Proof. Replacing x in (18) by $x + \Delta x$ we get

$$G(x + \Delta x) = \int_{x+\Delta x}^a f(t, x + \Delta x) dt. \tag{20}$$

If we take $t = z + \Delta x$, then (20) becomes

$$G(x + \Delta x) = \int_x^{a-\Delta x} f(z + \Delta x, x + \Delta x) dz. \tag{21}$$

By the Taylor series expansion of $f(z, x)$ around (z, x) we have

$$f(z + \Delta x, x + \Delta x) = f(z, x) + \left[\frac{\partial f(z, x)}{\partial z} + \frac{\partial f(z, x)}{\partial x} \right] \Delta x + h(z, x) \mathcal{O}(\Delta x^2). \tag{22}$$

Substituting (22) into (21) and doing some manipulations, we obtain

$$G(x + \Delta x) = \int_x^a f(z, x) dz - \int_{a-\Delta x}^a f(z, x) dz + \int_x^{a-\Delta x} \left\{ \left[\frac{\partial f(z, x)}{\partial z} + \frac{\partial f(z, x)}{\partial x} \right] \Delta x + h(z, x) O(\Delta x^2) \right\} dz. \tag{23}$$

Using (18) and (23), we get

$$\begin{aligned} \frac{G(x + \Delta x) - G(x)}{\Delta x} &= -\frac{1}{\Delta x} \int_{a-\Delta x}^a f(z, x) dz + \frac{1}{\Delta x} \int_x^{a-\Delta x} \left[\frac{\partial f(z, x)}{\partial z} + \frac{\partial f(z, x)}{\partial x} \right] dz \\ &\quad + \frac{O(\Delta x^2)}{\Delta x} \int_x^{a-\Delta x} h(z, x) dz. \end{aligned} \tag{24}$$

By the definition of derivative, we know that

$$\frac{dG(x)}{dx} = \lim_{\Delta x \rightarrow 0} \frac{G(x + \Delta x) - G(x)}{\Delta x}. \tag{25}$$

Since $\int_x^a \left[\frac{\partial f(z, x)}{\partial z} + \frac{\partial f(z, x)}{\partial x} \right] dz$ and $f(a, x)$ exist, we have

$$\lim_{\Delta x \rightarrow 0} \frac{1}{\Delta x} \int_{a-\Delta x}^a f(z, x) dz = f(a, x), \tag{26}$$

$$\lim_{\Delta x \rightarrow 0} \left(\int_x^{a-\Delta x} \left[\frac{\partial f(z, x)}{\partial z} + \frac{\partial f(z, x)}{\partial x} \right] dz \right) = \int_x^a \left[\frac{\partial f(z, x)}{\partial z} + \frac{\partial f(z, x)}{\partial x} \right] dz, \tag{27}$$

$$\lim_{\Delta x \rightarrow 0} \frac{O(\Delta x^2)}{\Delta x} \int_x^{a-\Delta x} h(z, x) dz = 0. \tag{28}$$

Using (25) and substituting (26)–(28) into (24) we get

$$\frac{dG(x)}{dx} = -f(a, x) + \int_x^a \left[\frac{\partial f(z, x)}{\partial z} + \frac{\partial f(z, x)}{\partial x} \right] dz. \quad \square \tag{29}$$

Application of the new formula (29) to (7) and (8) yields $\partial F / \partial \delta_0$ as follows:

$$\frac{\partial F}{\partial \delta_0} = -f(\delta_{cc}, \delta_0) + \frac{P_{\max 2}}{M} \int_{\delta_0}^{\delta_{cc}} (\sin \delta - \sin \delta_0) f^3(\delta, \delta_0) d\delta. \tag{30}$$

Substituting (12)–(15) and (30) into (11), we obtain the sensitivity of t_{cc} with respect to system load P_m as follows:

$$\begin{aligned} \frac{dt_{cc}}{dP_m} &= -f(\delta_{cc}, \delta_0) \left[\frac{1}{P_{\max 1} \cos \delta_0} + \frac{1}{(P_{\max 3} - P_{\max 2}) \sin \delta_{cc}} \left(\frac{P_{\max 2}}{P_{\max 1}} \tan \delta_0 + (\pi - \delta_3 - \delta_0) + \tan \delta_3 \right. \right. \\ &\quad \left. \left. - P_m \left(\frac{1}{P_{\max 1} \cos \delta_0} + \frac{1}{P_{\max 3} \cos \delta_3} \right) \right) \right] + \frac{1}{M} \int_{\delta_0}^{\delta_{cc}} \left[\frac{P_{\max 2} (\sin \delta - \sin \delta_0)}{P_{\max 1} \cos \delta_0} - (\delta - \delta_0) \right] f^3(\delta, \delta_0) d\delta. \end{aligned} \tag{31}$$

The sensitivity of critical clearing t_{cc} with respect to system load P_m could be utilized to determine t_{cc} approximately using Eq. (10) for small deviations in the system load while the system is operating a stable point P_{m0} . Such an approximation will evidently reduce the computation time when Monte Carlo simulation method is employed to obtain the PDF of t_{cc} . The procedure for applying Monte Carlo method to transient stability study is mainly composed of three parts. The first part simulates the occurrence of the uncertainties in system load. A random number generator is used to generate pseudo random numbers representing uncertain system load values. The second part is to calculate the critical clearing time t_{cc} based on every load value that is generated in the first part. In order to compute exact values of t_{cc} , Eq. (7) must be numerically solved for every load value, which is computationally expensive. However, Eq. (10) enables us to approximately calculate t_{cc} reducing computation time significantly. Based on the results from the second part, the third part calculates the histogram of exact or approximated t_{cc} . This histogram is then used to determine the probability of system being transiently stable using Eq. (1). The flow chart of the Monte Carlo simulation procedure is given in Fig. 5.

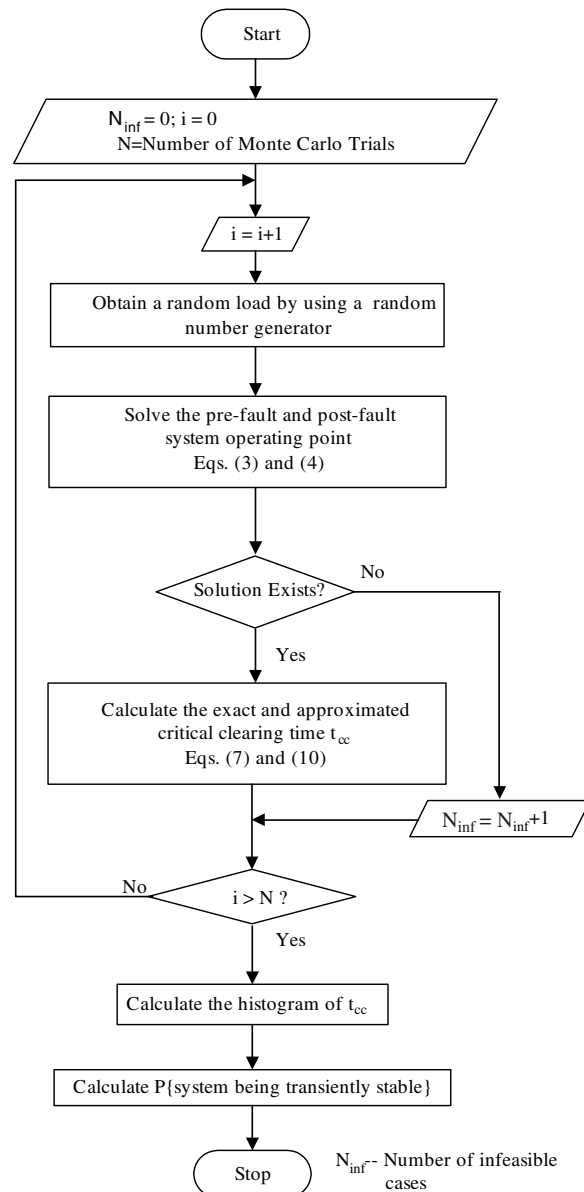


Fig. 5. Flow chart of Monte Carlo simulation.

5. Examples

The one-machine-infinite-bus (OMIB) system whose one-line diagram is given in Fig. 3 will be employed to verify the validity of the proposed linear approximation method in this section. The data of the OMIB system for pre-fault, fault-on and post-fault conditions is listed in Table 1.

Monte Carlo simulation has been performed with $N = 10^4$ independent random samples to estimate the PDF of both exact and approximated t_{cc} . In Monte Carlo simulations, Eq. (7) has been numerically integrated to compute exact values of t_{cc} while Eq. (10) together with Eq. (31) has been employed to determine the approximated values of t_{cc} . System load P_m is modeled as a Gaussian distribution random variable. Two different cases are chosen regarding to the mean value and standard deviation of this random variable. In both cases, deterministic values of the fault clearing time are used to determine the probability of the system being transiently stable.

Table 1
System parameters

	Pre-fault	Fault-on	Post-fault
M	0.01	0.01	0.01
E (pu)	1.11	0.1	1.11
V (pu)	1.0	1.0	1.0
X (pu)	0.5	0.5	1.0
P_{\max} (pu)	2.22	0.20	1.11

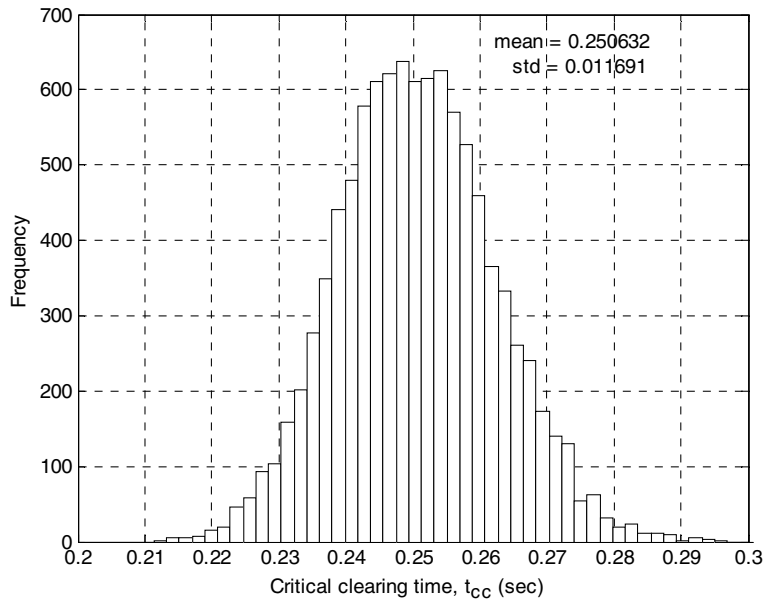


Fig. 6. Monte Carlo histogram of exact t_{cc} for Case 1.

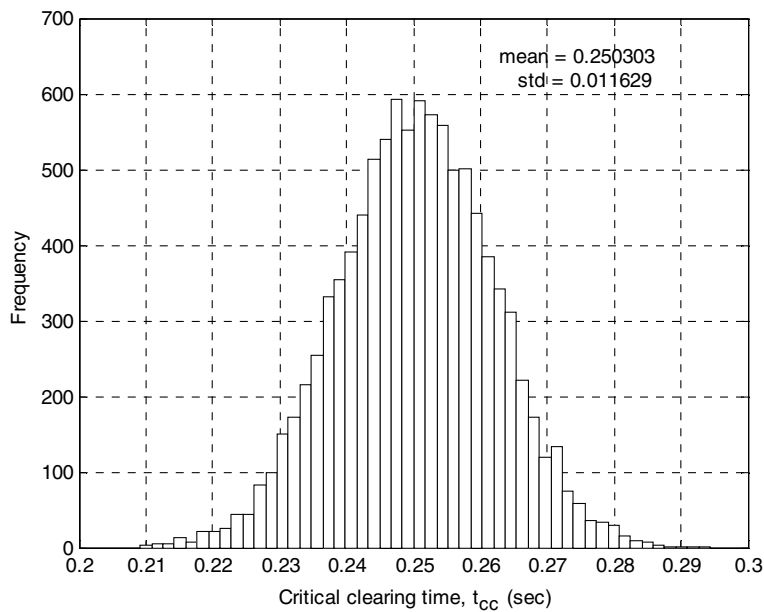


Fig. 7. Monte Carlo histogram of linearly approximated t_{cc} for Case 1.

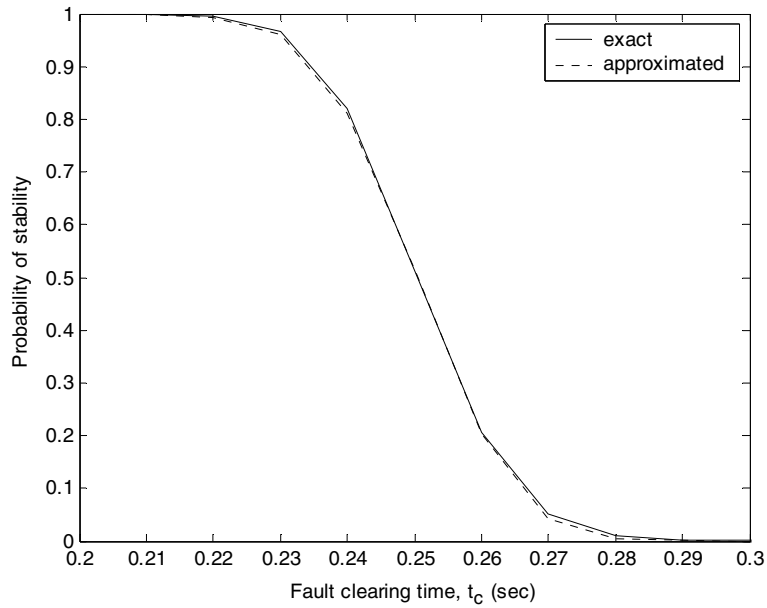


Fig. 8. Probability of system being transiently stable versus fault clearing time for Case 1.

5.1. Case 1

In this case, the mean value of P_m is assumed to be 0.5 pu while its standard deviation is 4% of its mean value. The Monte Carlo histograms of both the exact and linearly approximated t_{cc} 's are shown in Figs. 6 and 7, respectively. The probabilities of system being transiently stable at different levels of fault clearing time are calculated by applying Eq. (1) and the results are shown in Fig. 8.

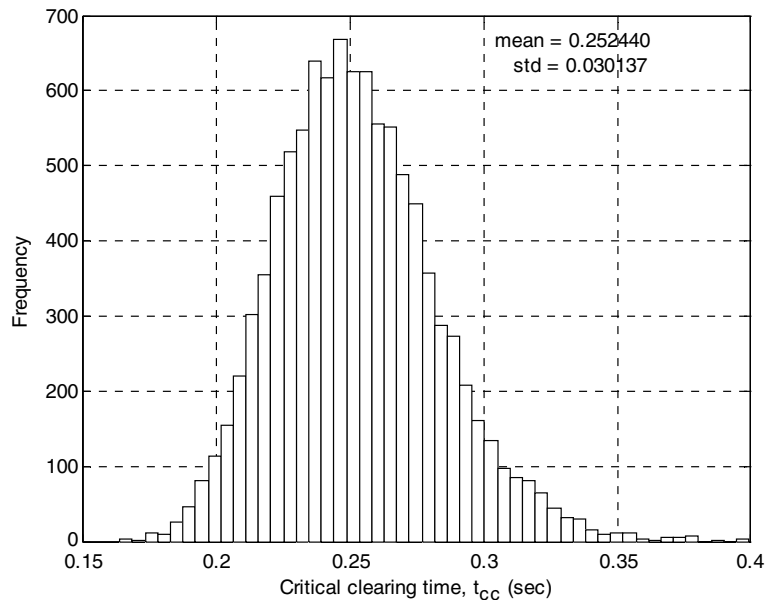


Fig. 9. Monte Carlo histogram of exact t_{cc} for Case 2.

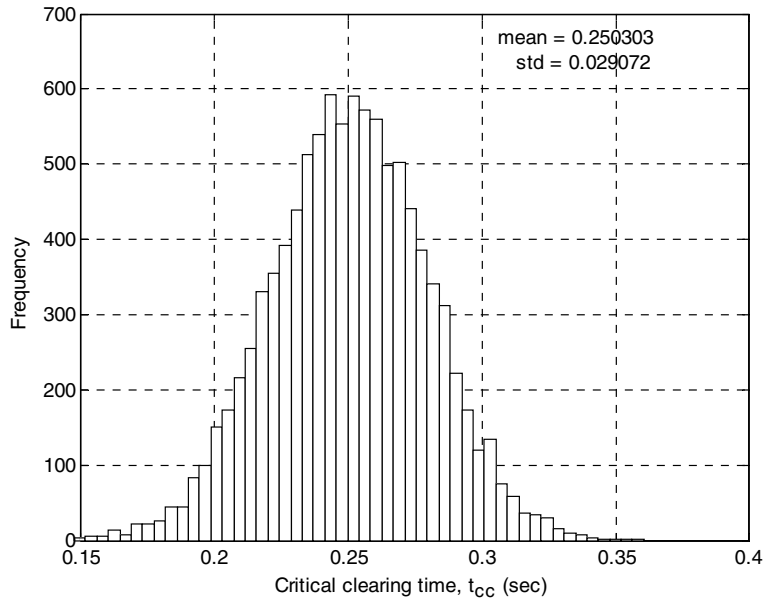


Fig. 10. Monte Carlo histogram of linearly approximated t_{cc} for Case 2.

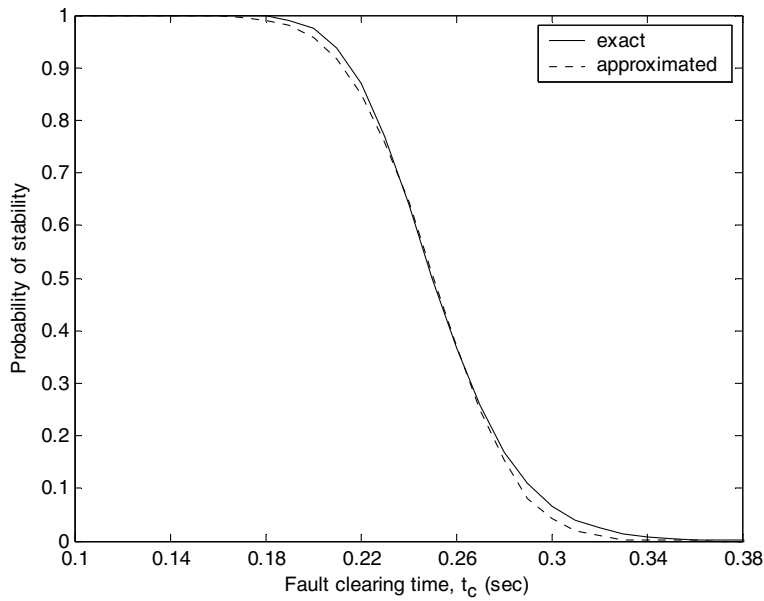


Fig. 11. Probability of system being transiently stable versus fault clearing time for Case 2.

5.2. Case 2

In this case, the mean value of P_m is assumed to be 0.5 pu while its standard deviation is 10% of its mean value. The calculations carried out in Case 1 are repeated in this case. The results are illustrated in Figs. 9–11.

Table 2
Mean and standard deviations of critical clearing time

Model	Case 1		Case 2	
	Mean	Standard deviation	Mean	Standard deviation
Exact	0.25063	0.01169	0.25244	0.03014
Linearly approximated	0.25030	0.01163	0.25030	0.02907

Table 3
Simulation times for $N = 10^4$ Monte Carlo samples

Model	Simulation times (s)	
	Case 1	Case 2
Exact	462.65	430.27
Linearly approximated	9.35	8.42

6. Discussions

Some observations from the results given in the previous section are listed and discussed in this section. Firstly, in case of small load deviations that corresponds to Case 1, by comparing the histogram of exact t_{cc} presented in Fig. 6 with that of approximated t_{cc} in Fig. 7 one can see that the proposed method correctly predicts the critical clearing time. This is even becomes more evident if one compares the mean and the standard deviation of critical clearing time for exact and linearly approximated methods. As Fig. 8 clearly illustrates, the probabilities of system being transiently stable (probability index) obtained by both the linear approximation method and the exact method are in close agreement, which verifies the accuracy of the proposed method for small load deviations.

Secondly, in case of large load deviations that corresponds to Case 2, the error gets relatively large. From Figs. 9 and 10 it is clear that the histograms of the exact t_{cc} and linearly approximated t_{cc} are not close any more. However, the mean and the standard deviation of t_{cc} 's determined by exact and approximated methods are significantly close. The comparison information on mean and standard deviations for both cases is summarized in Table 2. From Fig. 11, it is seen that the probabilities of system being transiently stable obtained by the linear approximation method departs from the exact ones especially when fault clearing time gets bigger. This is because of the fact that the linear approximation deteriorates when load deviation gets larger.

Thirdly, from Figs. 8 and 11 one can observe that in both cases the probabilities calculated by linear approximation method are always lower than the exact ones. In other words, the linear approximation method gives conservative results in these two cases. This is because of the fact that the approximated t_{cc} is always smaller than the accurate t_{cc} in both cases. The reason of this phenomenon is that the curve of t_{cc} versus P_m around an operating point is concave up.

Finally, computational times for exact and linear approximation models are summarized in Table 3 for both cases. As can be seen from this table, computational time decreases significantly when we implement the proposed method. It is clear from Table 3 that computational times of linearly approximated model is around 50 times less than those of the exact model for both cases, which is a very significant advantage of the proposed approximation for real-time on-line applications.

7. Conclusions

In this paper, the necessity of modeling the critical clearing time as a random variable in power system transient stability analysis is addressed. For the purpose of real-time on-line applications, a linear approximation method is proposed to reduce the complexity and computational time for obtaining the PDF of the critical clearing time. It is pointed out that the key issue in this method is the calculation of the sensitivity of the critical clearing time to the system load. A new formula is derived to overcome the difficulty of calculating this sensitivity. Monte Carlo simulations method is performed to estimate the PDF of the critical clearing time and

to validate the proposed method. Results from two cases for the OMIB power system show that the proposed method has significantly reduced the computational effort while the error remains relatively small. For the sake of illustration, in the paper reference has been made to a relatively simple power system. The extension of the proposed method to a multi-machine power system is presently under the study by the authors.

References

- [1] M. Pavella, P.G. Murthy, *Transient Stability of Power Systems: Theory and Practice*, John Wiley & Sons, 1994.
- [2] F. Wu, P. Varaiya, Direct methods for transient stability analysis of power systems: Recent results, *Proc. IEEE* 73 (12) (1985) 1703–1715.
- [3] A.A. Fouad, V. Vittal, *Power System Transient Stability Analysis using the Transient Energy Function Method*, Prentice-Hall, Englewood Cliffs, NJ, 1991.
- [4] H.-D. Chiang, C.-C. Chu, G. Cauley, Direct stability analysis of electric power systems using energy functions: Theory, applications, and perspective, *Proc. IEEE* 83 (11) (1995) 1497–1529.
- [5] H.-D. Chiang, F. Wu, P. Varaiya, Foundations of the potential energy boundary surface method for power system transient stability analysis, *IEEE Transactions on Circuits Systems* 35 (6) (1988) 712–728.
- [6] H.-D. Chiang, F. Wu, P. Varaiya, A BCU method for direct analysis of power system transient stability, *IEEE Transactions on Power Systems* 9 (3) (1994) 1194–1208.
- [7] Y. Xue, T.V. Cutsem, M. Ribbens-Pavella, Extended equal area criterion: justifications, generalizations, applications, *IEEE Transactions on Power Systems* 4 (1) (1989) 44–52.
- [8] M.H. Haque, Equal-area criterion: An extension for multi-machine power systems, *IEE Proc.-Generation Transmission Distribution* 141 (3) (1994) 191–197.
- [9] A.Z. Khan, F. Shahzad, A PC based software package for the equal area criterion of power system transient stability, *IEEE Transactions on Power Systems* 13 (1) (1998) 21–26.
- [10] R.G. Wasley, W.O. Stadlin, Network applications in energy management systems, *IEEE Computer Applications in Power* 4 (1) (1993) 31–36.
- [11] J.G. Anders, *Probability Concepts in Electric Power Systems*, John Wiley & Sons, New York, 1990.
- [12] R. Billinton, P.R.S. Kuruganty, A probabilistic index for transient stability, *IEEE Transactions on Power Apparatus and Systems* 99 (1) (1980) 195–206.
- [13] R. Billinton, P.R.S. Kuruganty, Probabilistic assessment of transient stability in a practical multimachine system, *IEEE Transactions on Power Apparatus and Systems* 100 (7) (1981) 3634–3642.
- [14] Y. Hsu, C. Chang, Probabilistic transient stability studies using the conditional probability approach, *IEEE Transactions on Power Systems* 3 (4) (1988) 1565–1572.
- [15] E. Chiodo, F. Gagliardi, D. Lauria, Probabilistic approach to transient stability evaluation, *IEE Proc.-Generation Transmission Distribution* 141 (5) (1994) 537–544.
- [16] E. Chiodo, D. Lauria, Transient stability evaluation of multimachine power systems: a probabilistic approach based on the extended equal area criterion, *IEE Proc.-Generation Transmission Distribution* 141 (6) (1994) 545–553.
- [17] F. Allella, E. Chiodo, D. Lauria, Transient stability probability assessment and statistical estimation, *Electric Power System Research* 67 (2003) 21–33.
- [18] S. Aboreshaid, R. Billinton, M. Fotuhi-Firuzabad, Probabilistic transient stability studies using the method of bisection, *IEEE Transactions on Power Systems* 11 (4) (1996) 1990–1995.
- [19] E. Chiodo, F. Gagliardi, M. La Scala, D. Lauria, Probabilistic on-line transient stability analysis, *IEE Proc.-Generation Transmission Distribution* 146 (2) (1999) 176–180.
- [20] E. Vaahedi, W. Li, T. Chia, H. Dommel, Large scale probabilistic transient stability assessment using B.C. Hydro's on-line tool, *IEEE Transactions on Power Systems* 15 (2) (2000) 661–667.
- [21] P.M. Anderson, A. Bose, A probabilistic approach to power system stability analysis, *IEEE Transactions on Power Systems* 102 (8) (1983) 2430–2439.
- [22] K.J. Timko, A. Bose, P.M. Anderson, Monte Carlo simulation for power system stability, *IEEE Transactions on Power Systems* 102 (10) (1983) 3453–3459.
- [23] A. Papoulis, *Probability, Random Variables, and Stochastic Processes*, McGraw-Hill, 1991.
- [24] F. Da-zhong, T.S. Chung, Dynamic single machine equivalent techniques for on-line transient stability assessment, *Electric Power System Research* 39 (1996) 179–186.
- [25] M. Pavella, Generalized one-machine equivalents in transient stability studies, *IEEE Power Engineering Review* (1) (1998) 50–52.
- [26] A.Z. Khan, Effects of power system parameters on critical clearing time: comprehensive analysis, *Electric Power System Research* 49 (1999) 37–44.
- [27] A.R. Bergen, V. Vittal, *Power System Analysis*, second ed., Prentice-Hall, Upper Saddle River, NJ, 2000.